Symposia on Turbulence in Liquids

Chemical and Biochemical Engineering

01 Sep 1969

The Response of a Hot-Wire Anemometer to a Bubble of Air in Water

S. C. Chuang

V. W. Goldschmidt

Recommended Citation

S. C. Chuang** and V. W. Goldschmidt***
Purdue University
Lafayette, Indiana

ABSTRACT

The sensitivity of peak voltage drop and duration of the change in sensor voltages due to the impaction of different size bubbles are computed and measured. Excellent agreement between these is found for bubbles somewhat larger than the sensor diameter and smaller than its effective length in water streams in a range of 1.5 to 9 feet per second. The method suggests a reliable method for sizing bubbles in a water stream. The effects due to nondirect hits are not treated.

INTRODUCTION

Undoubtedly, the most common villain to researchers attempting to measure turbulence in water has been the presence of air bubbles. Akin to dust in air, they many times become the scapegoat for poor calibration curves, and hence, unreliable measurements.

In the work reported herein bubbles were purposely introduced in a water jet. Their dispersion was of interest; hence, a means of determining their concentration and size distribution was necessary. Earlier work [1,2] had already extended the use of the hot-wire anemometer as an aerosol sampler; now the purpose was to employ it as a bubble sampler, both in size and concentration. The work presented herein treats the former and in particular, the nature of the signal due to the traverse of a bubble past the sensor.

The bubbles may be classified into three groups of sizes according to their behavior when approaching the wire. In the first group are those which are of a diameter in the order of 4 times the sensor's diameter or smaller. These will tend to avoid impaction with the sensor, or to roll off without breaking when impacting. This is due to the pressure field caused by the curving streamlines. The second group is that of bubbles whose diameter is in the order of magnitude of the sensor's length or larger. These will in general tend to change shape and distort into an unpredictable geometry when hitting the sensor. It is the group of bubbles whose size is somewhat larger than the wire diameter and smaller than its length to which our attention is limited. It has been found that bubbles ranging from about 4 times to at least 20 times the sensor's diameter, behave in an orderly and predictable manner when impacting directly on the conventional cylindrical sensor.

In the reported work the effect of partial hits or bubbles hitting at a glance is not treated. In essence this means that the sample curves of

Figure 1 are assumed to be rectangular in shape. This is a strong limitation to the sampler. To necessarily improve from this assumption, the actual pathline geometry has to be determined. The assumption is tantamount to considering only bubbles directly aimed towards the sensor.

A bubble when hitting the wire will change the heat transfer characteristic and hence cause a change in the wire voltage [3]. The wire voltage drop will change as shown in Figure 2. The voltage drop corresponds to a decrease in cooling for a constant temperature anemometer. The time of traverse, t, and peak voltage drop of the signal, E_p, are related to the bubble size, d_b, and the stream velocity, V. In the above, E_p is defined as the difference of the maximum and minimum values of the voltage across the wire during the bubble impaction. The relationship among d_b, E_p, t_b, and V (if defined) would then permit measurement of the bubble size as well as bubble concentration in the bubble-water two-phase flow from a simple analysis of the cooling signal.

THEORETICAL RESPONSE

Two different criteria, as suggested in Figure 2, may be used for measuring bubble size. One is the time of traverse and the other the peak voltage drop. Correspondingly two coefficients of sensitivity can be defined.
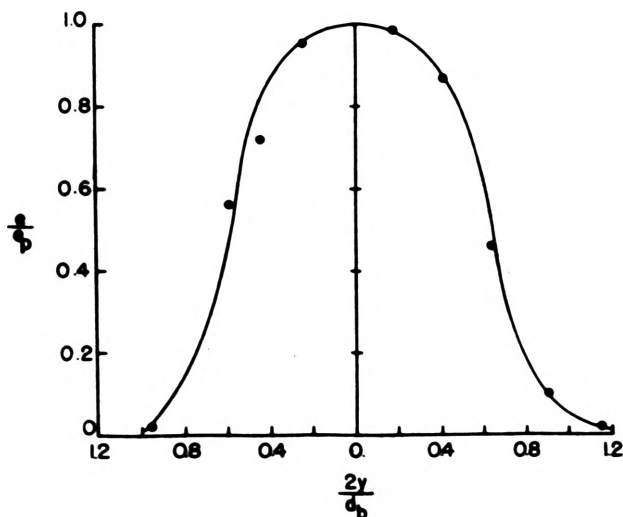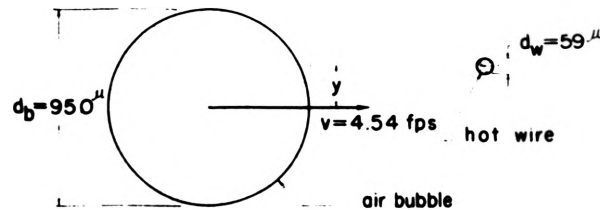

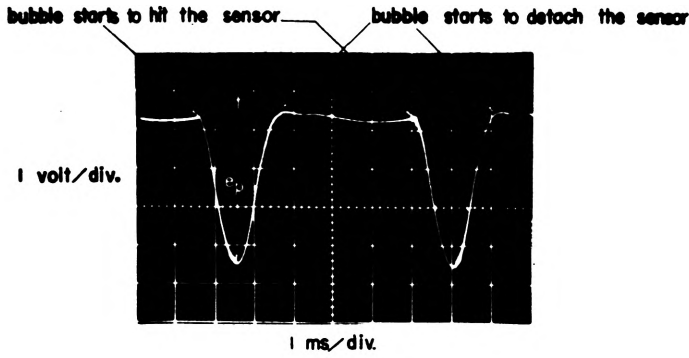FIG.1. PARTIAL HIT EFFECT

I volt/div.

e_b

I ms/div.

FIG. 2 TYPICAL DECREASE IN COOLING DUE TO BUBBLE

Consider the first, i.e., $d(t_b)/d(d_b) = S_t$. Assume that the bubble moves with the same velocity as the carrier stream, and remains in a spherical shape even while engulfing and passing the wire. The relationship of t_b, d_b, d_w and V_b will simply be

$$t_b = \frac{d_b + d_w}{V_b} \qquad (1)$$

where d_w is the cylindrical sensor diameter. The sensitivity S_t becomes simply

$$S_t = 1/V_b \qquad (2)$$

Consider the second, i.e., $d(E_p)/d(d_b) = S_E$. The instaneous voltage across the wire is a function of time

$$E(t) = I(t) R \qquad (3)$$

where $E(t)$, $I(t)$ and R are voltage, current and resistance at time, t. Note that since a constant temperature anemometer is used then R, for a fixed overheat ratio, has a constant value.

The total Joulean heat of the wire, $I^2(t)R$, is equal to the heat per unit time transferred to the air bubble and to the water from the sensor. Once the heat transfer characteristic of the wire is known, $I(t)$ can be obtained, and $E(t)$ can be calculated from equation (3).

The assumed geometry, at a time t, when the bubble directly engulfs the middle of the wire is shown in Figure 3. ℓ is the effective length of the wire, r_b is the bubble radius and $f(t)$ is the half length of the wire exposed to air phase. The latter is a function of t and bubble velocity V,

$$f(t) = [r_b^2 - (r_b - Vt)^2]^{1/2} \qquad (4)$$

The energy conservation equation neglecting free convection effects reads

$$I^2(t) \, r(y,t) = C_w \frac{\partial T_w(y,t)}{\partial t} - K \frac{\partial^2 T_w(y,t)}{\partial y^2}$$
$$+ a_1[T_w(y,t) - T_b(t)] \qquad (5a)$$

for the part of the wire exposed to the air phase and

$$I^2(t) \, r(y,t) = C_w \frac{\partial T_w(y,t)}{\partial t} - K \frac{\partial^2 T_w(y,t)}{y^2}$$
$$+ a_2[T_w(y,t) - T_e] \qquad (5b)$$

for the part of the wire exposed to the water phase. The left hand side of equations (5a) and (5b) is the rate of the thermal energy production per unit length of the wire at position y (measured axially along the wire) and at time t. $r(y,t)$ is the electric resistance per unit length at position y

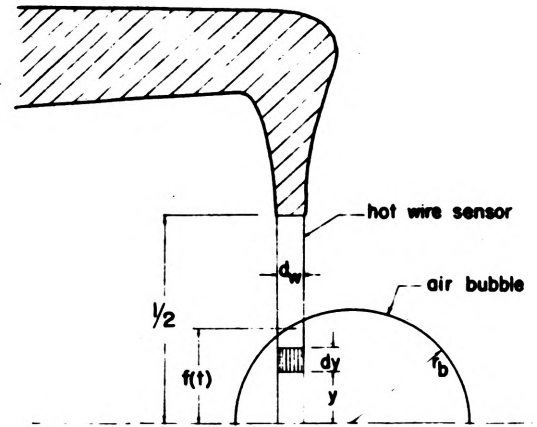## FIG. 3-a ASSUMED GEOMETRY OF IMPACTION

hot wire sensor
air bubble
d_w
$\ell/2$
$f(t)$
dy
y
r_b

heat flow out due to
axial conduction

heat conducted
away due to
forced convection

heat stored inside the element

Joulean heat production
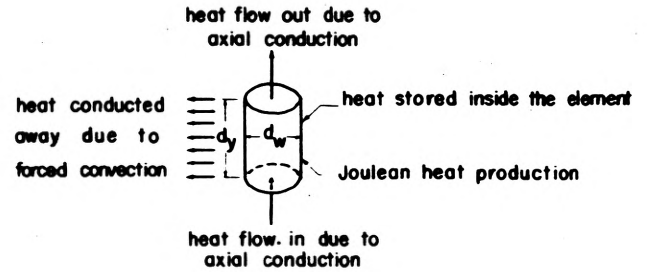
d_y d_w

heat flow in due to
axial conduction

FIG. 3-b ENERGY BALANCE OF A FINITE WIRE ELEMENT

and at time t. It is linearly related to the wire temperature, $T_w(y,t)$,

$$r(y,t) = r_o[1 + b(T_w(y,t) - T_o)] \qquad (6)$$

where $T_w(y,t)$ is the wire temperature at position y and at time t, r_o is the resistivity per unit length of the wire at temperature T_o and b is the temperature coefficient of the electrical resistivity.

The first term in the right hand side of equations (5a) and (5b) is the unsteady term, where C_w is the wire specific heat.

The second term in the right hand side of equations (5a) and (5b) is the rate of heat conduction in the axial direction; here K is the corresponding thermal conductivity.

The third term in the right hand side of equations (5a) and (5b) corresponds to the forced convection. $T_b(t)$ is the temperature within the bubble, T_e is the surrounding water temperature, and a_1 and a_2 are the heat transfer coefficients per unit length of the wire exposed to the air and to the water phases, respectively. All of the above coefficients can be easily defined except for a_1, a_2 and $T_b(t)$. The bubble temperature is assumed homogeneous and hence dependent on time only.

For the case where the wire element is exposed to the air phase, a_1 may be expressed as

$$a_1 = \frac{Nu_1 \, k_1}{d_w} \pi d_w = \pi Nu_1 \, k_1 \qquad (7)$$

where k_1 is the heat conduction coefficient of the air at the film temperature and Nu_1 is the Nusselt number. The Nusselt number is a function of the Prandtl and Reynolds numbers. It is calculated at the film temperature,

$$T_{f_1} = \frac{1}{2} [T_w(y,t) + T_b(t)] \qquad (8)$$

For air flow over the wire, the Nusselt number may be expressed as[4]

$$Nu_1 = C + D \ Re_1^n \left[\frac{T_{f_1}}{T_b(t)}\right]^{0.17} \qquad (9)$$

The coefficients C and D and the exponent n are dependent on the Reynolds number. For Reynolds numbers between 2 and 20, they become C = 0.24, D = 0.56 and n = 0.45.

For the case where the wire element is exposed to the water phase, a_2 is expressed as

$$a_2 = \frac{Nu_2 \ k_2}{d_w} \pi d_w = \pi Nu_2 \ k_2 \qquad (10)$$

where k_2 is heat conduction coefficient of the water at the film temperature and Nu_2 is Nusselt number calculated at the film temperature,

$$T_{f_2} = \tfrac{1}{2}[T_w(y,t) + T_e]. \qquad (11)$$

Eckert and Drake[5] suggest that

$$Nu_2 = 0.43 + 0.534 \ Pr_2^{0.31} \ Re_2^{0.5}$$
$$\text{for } 1 < Re_2 < 4,000 \qquad (12)$$

Equations (7) through (12) give then valid empirical values for the coefficients a_1 and a_2 of equations (5a) and (5b). One other term deserving further consideration is $T_b(t)$. It appears in the last term of equation (5a), making equation (5a) much more complicated than (5b) due to the additional time dependence. In order to account for this, a quasi-steady case is assumed where the temperature distribution inside the air bubble is considered uniform at a certain instant during the heating process. Equating the time rate of change of heat inside the bubble with that transferred per unit time from the wire segment in contact with the bubble itself then

$$\frac{d}{dt} \ [\frac{4 \ r_b^3 \ \rho_a}{3} \ C_a T_b(t)] = \int_{-f(t)}^{f(t)} a_1[T_w(y,t) - T_b(t)]dy \qquad (13)$$

In the above ρ_a is the density, C_a is the specific heat of the air, and f(t) is as defined in equation (4).

Equations (5a) and (5b) together with (6) through (13) comprise now a complete system of linear partial differential equations. Together with the constant temperature operation requirement that

$$\int_{-\ell/2}^{\ell/2} r(y,t) \ dy = R \qquad (14)$$

a numerical solution and evaluation of the sensitivity, S_E can be made. Details of the computer solution are not given in this paper; however, they will be part of the first author's Ph.D. thesis.

Figure 4 is a typical voltage versus time curve; and, it is for a 400 micron bubble in a 4 fps stream. The abscissa is plotted as a dimensionless time, Vt/V_b. Similarity with the oscillograph of Figure 2 is not seen in the somewhat skewed calculated signal of Figure 4.

Figure 5 shows the computed sensitivity S_E, relating the voltage to the bubble size. The peak voltage increases with bubble size and decreases with velocity. A simple functional relationship for S_D, as that for S_t (equation (2)), is not possible although its value may be obtained from a family of curves such as those in Figure 5.

Experimental Setup

A Thermosystem (Model 1217-20) hot film probe was used. The wire diameter, d_w, and effective length, ℓ, were measured as 59 and 1324 microns, respectively. The cross-section of the wire, according to the manufacturers is adequately described by Figure 6b. The flow field consisted of a submerged circular jet. The diameter of the jet orifice was 1/2 inch. The exit velocity of the carrier stream ranged from 1.5 fps to 12 fps. All measurements were taken in the potential core. The schematic diagram of the flow field is shown in Figure 6a and 6c. Bubbles of three different sizes were generated by applying a fixed air pressure through a small syringe tube placed just upstream of the jet orifice. The inner diameter of the syringe tube nozzle was of 28 microns. The bubbles generated were measured in the moving stream photographically as 400μ, 950μ and 1300μ. These sizes were also checked by measuring the rise time of the bubbles in a quiescent stream. The hot-wire sensor was carefully placed in the potential core of the jet in such a manner that the bubbles hit directly upon it. Direct hitting was ascertained by monitoring the output signal on the oscilloscope while adjusting the location of the sensor.

Test and Results

The time of bubble traverse, t, and the peak voltage drop E_p, were measured from oscilloscope pictures as that shown in Figure 2. As a further example the corresponding signals for a 400 micron bubble hitting the wire at different velocities are shown in Figures 7a through 7f. The changes in the shape of the signal with an increase of bubble velocity bring about some uncertainty when measuring the traverse time for bubble velocities greater than 9 fps.

The corresponding measured relationship between t and d_b is shown in Figure 8. The results are valid only for velocities ranging from 1.5 fps to 9 fps. The theoretical relationship between t and d_b was given by equation (1). It is plotted on Figure 8 as a dashed line showing excellent agreement.

The corresponding relationship between E_p and d_b, as measured from the oscilloscope pictures are shown surperposed on the theoretical plots of Figure 5
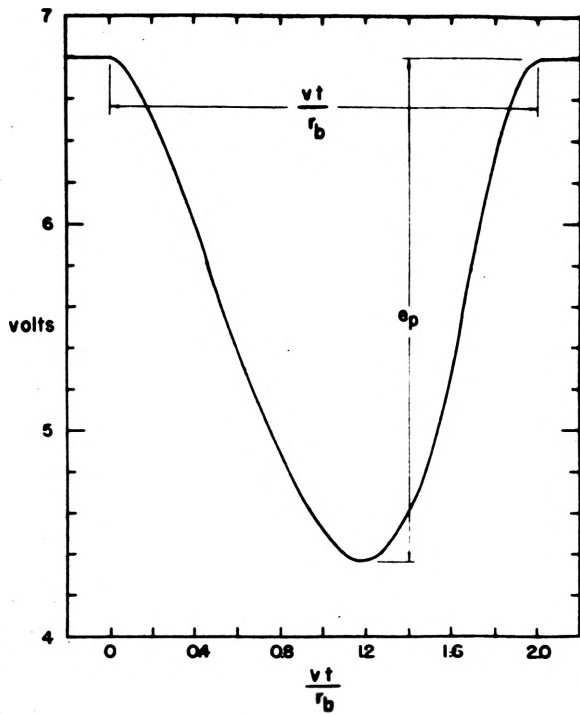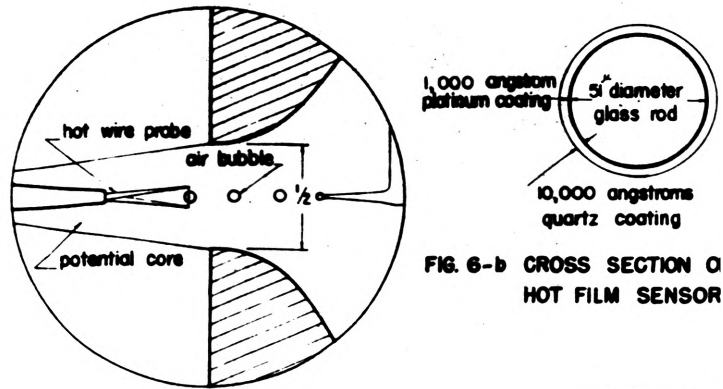
FIG. 4 TYPICAL VOLTAGE VS. TIME (CALCULATED)

$\dfrac{vt}{r_b}$

e_p

volts

FIG. 6-b CROSS SECTION O
HOT FILM SENSOR

1,000 angstrom platinum coating

5" diameter glass rod

10,000 angstroms quartz coating

hot wire probe

air bubble

potential core

½

FIG. 6-c DETAILED SKETCH AT POTENTIAL CORE

elevated tank

hot wire

syringe tube

honey comb

jet tank

reservoir

pump
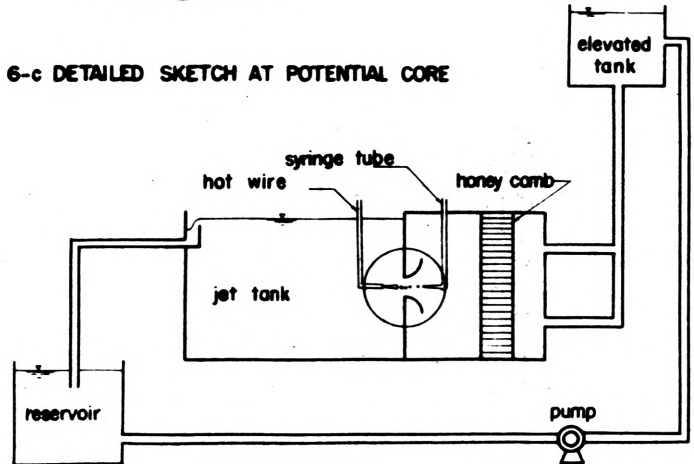
FIG. 6-a SCHEMATIC DIAGRAM OF FLOW FIELD

v = 3 f p s
v = 4 f p s
v = 5 f p s
v = 6 f p s
v = 8 f p s

e_p
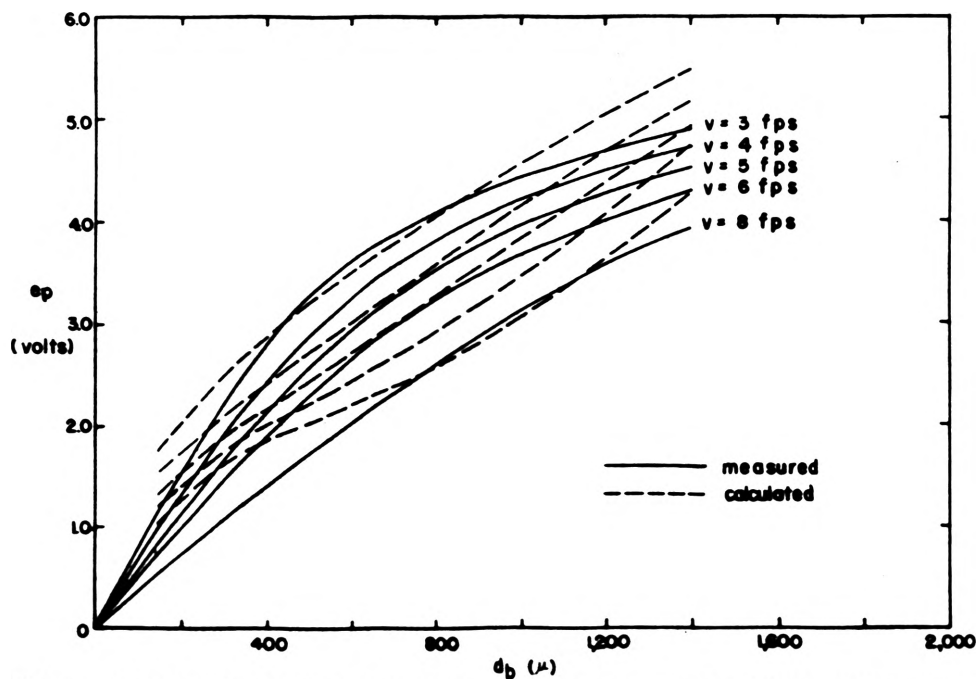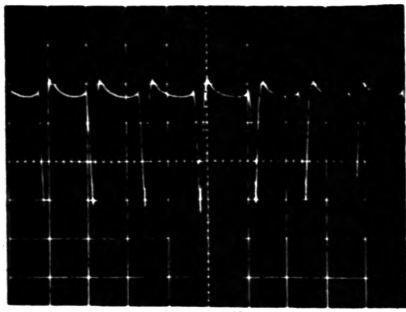(volts)

measured
calculated

d_b (μ)

FIG. 5 PEAK VOLTAGE DROP VS. BUBBLE DIAMETER (CALCULATED & MEASURED)

1.5 volt/div.

2 ms/div.

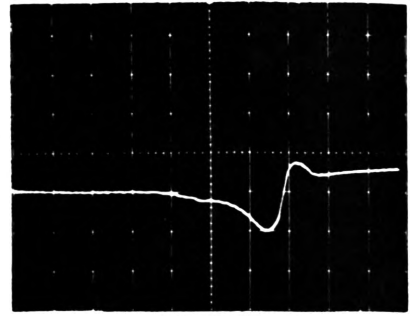FIG. 7-a $d_b = 400^\mu$, $v_b = 1.5$ fps

1 volt/div.

0.2 ms/div.

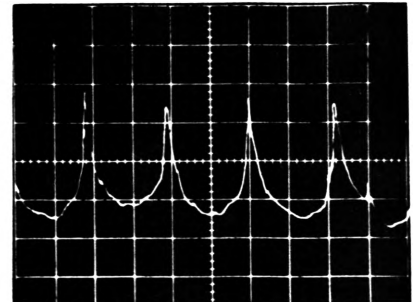FIG. 7-b $d_b = 400^\mu$, $v_b = 3.07$ fps

0.5 volt/div.

0.05 ms/div.

FIG. 7-e $d_b = 400^\mu$, $v_b = 14$ fps

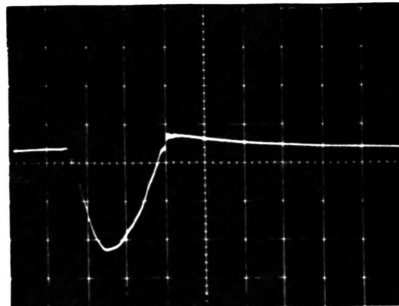2 volt/div.

1 ms/div.

FIG. 7-f $d = 2,500^\mu$, $v = 2.2$ fps

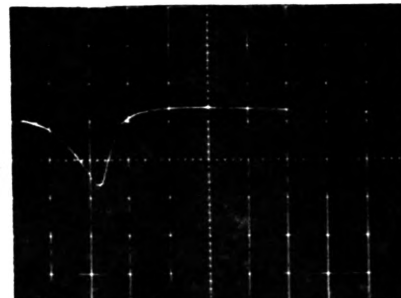FIG. 7 SIGNALS OF VARIOUS VOLTAGE OUTPUTS

0.8 volt/div.

2 ms/div.

FIG. 7-c $d_b = 400^\mu$, $v_b = 5.5$ fps

0.5 volt/div.

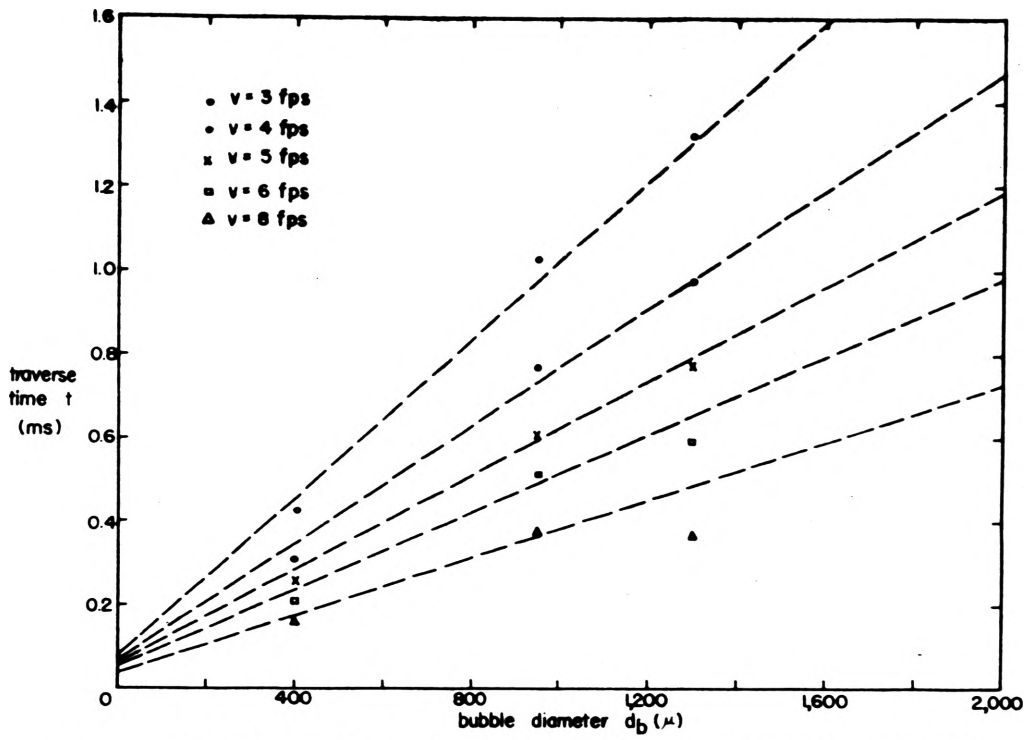0.05 ms/div.

FIG. 7-d $d_b = 400^\mu$, $v_b = 9.78$ fps

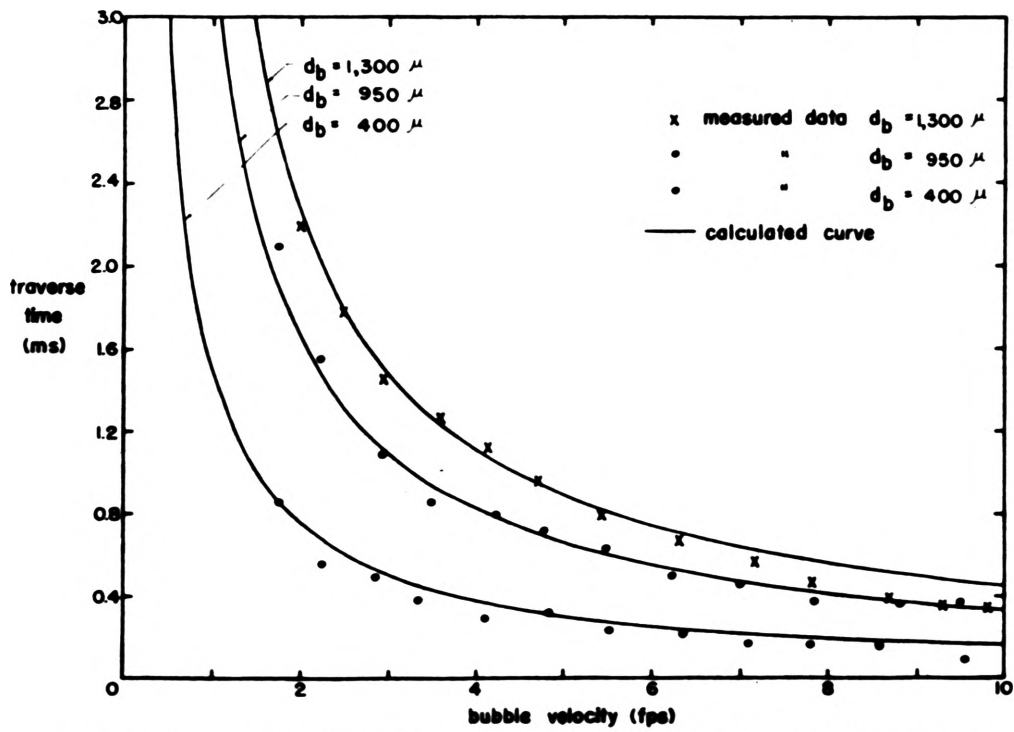FIG. 8   TRAVERSE TIME VS. BUBBLE DIAMETER (CALCULATED & MEASURED)

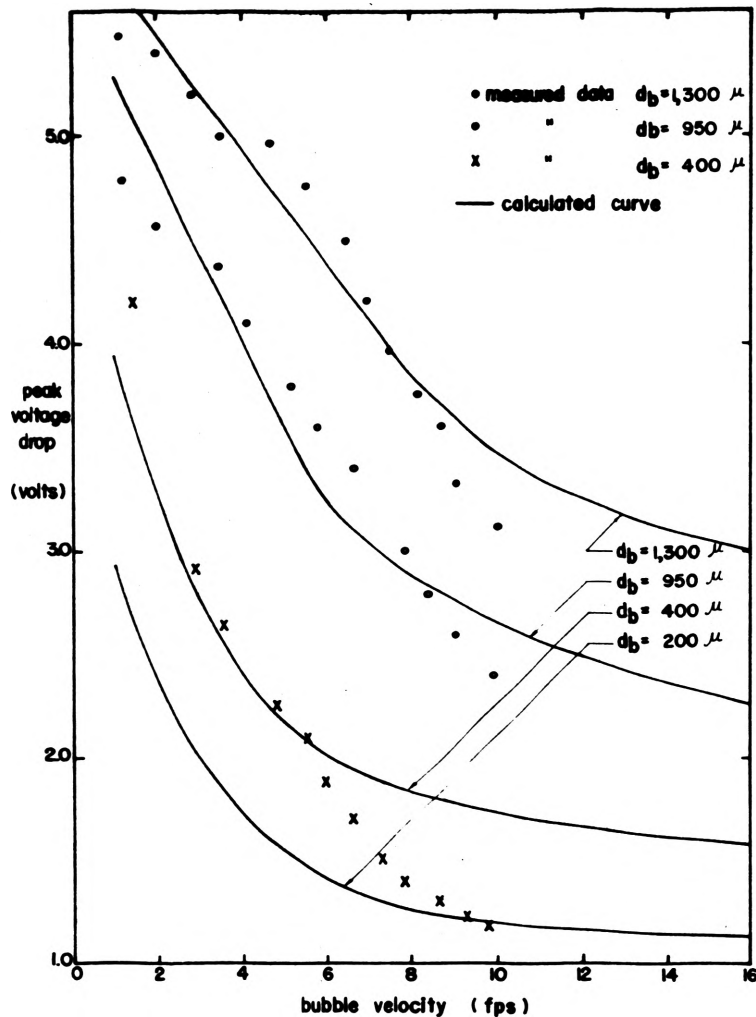FIG. 9   TRAVERSE   TIME   VS.   BUBBLE VELOCITY (CALCULATED & MEASURED)

FIG. IO PEAK VOLTAGE DROP VS. BUBBLE VELOCITY (CALCULATED & MEASURED)

The agreement is not too good for the larger drops whose diameter is in the order of the wire length. For these the model proposed would obviously fail, but it is very good for the group of particles to which the analysis was limited.

The experiment as performed did not permit wide variations in bubble size. A further comparison between theory and measurements is possible when comparing traverse time and peak voltage with mean velocity for the three different bubble sizes. Comparisons of this type are shown in Figures 9 and 10. From Figures 9 and 10 it is seen that the agreement between the measured data and the calculated values is good within mean velocities from 1.5 fps to 8 fps, accordingly validating the model proposed.

CONCLUSIONS

The results have clearly shown that bubbles of a certain size range may be effectively sampled as to their size with a simple hot-wire anemometer. For this particular case (Thermo-System 1217-20 sensor) bubble sizes between 400 to 1300 microns in a stream with velocities between 1.5 to 8 fps, gave signals whose amplitude and duration were a direct measure of bubble size. An analysis based on the assumption that the bubbles engulfed and passed the sensor with their shape and velocity unchanged gave good agreement with measured values.

SYMBOLS

a_1, a_2	heat transfer coefficients per unit length of the sensor exposed to air and water phase, respectively
b	temperature coefficient of electrical resistivity
c	empirical coefficients
C_w	specific heat per unit length of the sensor
D	empirical coefficient in Eq. (9)
d_b	bubble diameter
d_w	sensor diameter
E_p	peak voltage drop
$E(t)$	instantaneous voltage across the sensor
$f(t)$	half length of the wire exposed to the air bubble phase
$I(t)$	instantaneous current across the sensor
k	axial thermal conductivity of the sensor
k_1, k_2	heat conduction coefficients of the air and of the water at the film temperature
ℓ	effective length of the sensor
Nu_1, Nu_2	Nusselt numbers for sensor exposed to air and water phase, respectively
n	exponent in Eq. (9)
Pr_2	Prandtl number
R	total sensor resistance
rb	bubble radius
$r(y,t)$	electrical resistivity at position y and at time t
r_o	electrical resistivity of the sensor at temperature T_o
S_E	sensitivity based on the peak voltage drop E_p
S_t	sensitivity based on the traverse time t
$T_b(t)$	instantaneous bubble temperature
T_{f_1}, T_{f_2}	film temperature of sensor exposed to air and water phase, respectively
T_e	ambient temperature
$T_w(y,t)$	sensor temperature at position y and at time t
t_b	traverse time of a bubble
t	time
V	stream velocity
V_b	bubble velocity
y	coordinate in the axial direction of the sensor
ρ_a	air density

REFERENCES

1. Goldschmidt, V. W., "Measurement of Aerosol Concentrations with a Hot-Wire Anemometer," J. Colloid Sci., 20, 617-634 (1965).

2. Goldschmidt, V. W., and Householder, M. ,.: "Measurement of Aerosols by Hot-Wire Anemometry," AFOSR Final Report, AFOSR No. 68-1492, pp. 134-152, July 1968.

3. Hsu, Y. Y., Simon, F. F., Graham, R. W.: "Application of Hot-Wire Anemometry for Two-Phase Flow Measurements such as Void Fraction and Slip Velocity," ASME Winter Meeting, Philadelphia, Pennsylvania, November 1963.

4. Collis, D. C., and Williams, M. J., "Two-Dimensional Convection from Heated Wires at Low Reynolds Number," J. Fluid Mech., 6, 357-384 (1959).

5. Eckert, E. R. G., and Drake, Robert M., Jr., Heat and Mass Transfer, McGraw-Hill Book Co., Inc., New York, 1959.